

Published in final edited form as:

Nat Struct Mol Biol. ; 18(9): 1052–1059. doi:10.1038/nsmb.2108.

Mechanism of ubiquitylation by dimeric RING ligase RNF4

Anna Plechanovová¹, Ellis G. Jaffray¹, Stephen A. McMahon², Kenneth A. Johnson², Iva Navrátilová³, James H. Naismith², and Ronald T. Hay¹

¹Wellcome Trust Centre for Gene Regulation and Expression, College of Life Sciences, University of Dundee, Dundee, UK

²Biomedical Sciences Research Complex, University of St. Andrews, St. Andrews, UK

³Division of Biological Chemistry and Drug Discovery, College of Life Sciences, University of Dundee, Dundee, UK

Abstract

Mammalian RNF4 is a dimeric RING ubiquitin E3 ligase that ubiquitylates poly-SUMOylated proteins. We found that RNF4 bound ubiquitin-charged UbcH5a tightly but free UbcH5a weakly. To provide insight into the mechanism of RING-mediated ubiquitylation we docked the UbcH5~ubiquitin thioester onto the RNF4 RING structure. This revealed that with E2 bound to one monomer of RNF4, the thioester-linked ubiquitin could reach across the dimer to engage the other monomer. In this model the “Ile44 hydrophobic patch” of ubiquitin is predicted to engage a conserved tyrosine located at the dimer interface of the RING and mutation of these residues blocked ubiquitylation activity. Thus, dimeric RING ligases are not simply inert scaffolds that bring substrate and E2-loaded ubiquitin into close proximity. Instead, they facilitate ubiquitin transfer by preferentially binding the E2~ubiquitin thioester across the dimer and activating the thioester bond for catalysis.

Introduction

Ubiquitin conjugation is a widely utilized and highly flexible means of altering the fate of target proteins. Ubiquitin is first activated by formation of a thioester bond between its C-terminus and a cysteine residue of the E1 activating enzyme. It is then transferred to an E2 conjugating enzyme, again forming a thioester bond with the active site cysteine residue. Ubiquitin transfer is accomplished when the ϵ -amino group of a lysine side chain in the target protein attacks the thioester yielding an isopeptide bond. This final step is usually catalyzed by a ubiquitin E3 ligase that recruits both the E2~ubiquitin (E2~Ub) thioester and the specific substrate^{1,2}. There are two broad classes of ubiquitin E3 ligases: Homologous to E6-AP C-Terminus (HECT) ligases and Really Interesting New Gene (RING) ligases³. HECT-type ubiquitin E3 ligases contain a catalytic cysteine residue that forms a thioester intermediate with ubiquitin before final transfer¹. RING E3 ligases do not form a covalent intermediate, but catalyze direct transfer of ubiquitin from the E2~Ub thioester to a substrate.

Correspondence should be addressed to R.T.H. (r.t.hay@dundee.ac.uk).

Accession codes. Protein Data Bank: Coordinates and structure factors for the RING domain of RNF4 have been deposited under accession code 2XEU.

Author contributions A.P. purified RNF4 proteins, carried out crystallography, conducted biochemical analysis and interpreted the data. E.G.J. purified recombinant proteins and carried out ubiquitylation assays. S.A.M., K.A.J. and J.H.N. contributed to structural analysis. I.N. contributed to biochemical analysis. A.P., J.H.N. and R.T.H. wrote the paper. R.T.H. conceived the project and contributed to data interpretation.

RING proteins contain a conserved arrangement of cysteine and histidine residues that coordinate two zinc atoms and cross-brace the folded structure.

Like ubiquitin, Small Ubiquitin-like MOdifier (SUMO) functions as a posttranslational modification of other proteins⁴. SUMO-Targeted Ubiquitin Ligases (STUbLs) are a conserved family of proteins that target SUMO modified proteins for ubiquitylation⁵⁻¹⁰, as typified by RING Finger Protein 4 (RNF4) in mammals¹¹⁻¹³. STUbLs contain multiple SUMO-Interaction Motifs (SIM)¹⁴⁻¹⁶ and a RING domain, allowing them to specifically recognize poly-SUMO chains. In response to arsenic therapy the Promyelocytic Leukaemia Protein (PML) is modified with a poly-SUMO chain that recruits RNF4, thus targeting the modified protein for ubiquitin mediated degradation^{12,13}.

To determine the mechanism of RING mediated ubiquitylation, we first obtained the structure of the homodimeric RNF4 RING domain from *Rattus norvegicus*. To probe the role of dimerization in RING function, we docked E2~Ub thioester onto the experimental structure of the RNF4 RING domain. The model shows the E2 bound to one monomer, while the thioester-linked ubiquitin engages the other monomer, potentially rationalizing the requirement for the dimer. The predicted interface between ubiquitin and RNF4 centres on the “Ile44 hydrophobic patch” of ubiquitin and conserved Tyr193 of the RNF4 RING. Mutation of these residues abolished the preferential interaction between the RING domain and ubiquitin-loaded E2 and abrogated ubiquitin E3 ligase activity. Thus, dimeric RING ligases such as RNF4 do not act as an inert scaffold, but mediate catalysis by binding E2~Ub thioester, activating the thioester bond and thus allowing efficient transfer of ubiquitin to substrate.

Results

RNF4 RING domain is sufficient for ubiquitylation activity

RNF4 possesses a C-terminal RING domain required for ubiquitin E3 ligase activity¹³, whilst four tandem SUMO-interaction motifs (SIMs) located in the N-terminal region provide specificity for binding to its substrate, poly-SUMO chains (Supplementary Fig. 1a,b). In the absence of a substrate, RNF4 attaches ubiquitin to its internal lysine residues (autoubiquitylation). The isolated RING domain of RNF4 was active in autoubiquitylation, confirming the RING domain is sufficient for ubiquitin transfer (Supplementary Fig. 1c). However, it was unable to ubiquitylate poly-SUMO-2 chains (Supplementary Fig. 1d). We generated a linear head-to-tail fusion of four SUMO-2 molecules (termed 4 × SUMO-2) as a model substrate for RNF4, since longer poly-SUMO chains (N > 4) are efficiently ubiquitylated by RNF4 (ref. 13). 4 × SUMO-2 undergoes RNF4 dependent ubiquitylation with similar efficiency as isopeptide bond-linked SUMO-2 tetramers (Supplementary Fig. 2).

To study the mechanism of RNF4-mediated ubiquitylation, we established a single-turnover substrate ubiquitylation assay in which E2 (UbcH5a) was first charged with ubiquitin in the absence of substrate and E3. ATP was then depleted by adding apyrase to stop further E1-mediated loading of E2. Subsequently, RNF4 and substrate were added to initiate transfer of ubiquitin from E2 to substrate. ¹²⁵I-labeled 4 × SUMO-2 was efficiently ubiquitylated by RNF4 (Fig. 1a,b). Moreover, with the two substrates (4 × SUMO-2 and E2~Ub) in excess, the reaction rate is linearly dependent on the concentration of RNF4.

RNF4 residues required for dimerization and E2 binding

As a first step in understanding RNF4-catalyzed ubiquitylation, we determined a 1.5 Å resolution crystal structure of the RING domain of RNF4 (Table 1, Supplementary Fig. 3), which adopts a typical RING fold stabilized by two zinc ions co-ordinated by one histidine

and seven cysteine residues. The RING domain crystallized in space group $P4_132$ with one monomer in the asymmetric unit, but was dimeric in solution (Supplementary Fig. 4). In the crystal, the two subunits of a dimer are related by a crystallographic two-fold axis (Fig. 1c). This is consistent with a recently published structure for RNF4 RING domain¹⁷

The dimer interface is formed mainly by residues from the three β -strands together with residues at the very C-terminus of RNF4 (Fig. 1d). In total, dimerization buries 518 Å² of surface accessible area of a monomer. The aromatic ring of Tyr193 appears to shield the dimer interface while a hydrogen bond between the amide nitrogen of Tyr193 and the carbonyl oxygen of Gly159 in the other subunit bridges the two monomers. Mutation of residues at the dimer interface (Val161, His190, Ile192, Tyr193, and Ile194; Fig. 1d) disrupted dimerization (Supplementary Fig. 5). Monomeric RNF4 mutants were inactive and only at ten times higher RNF4 concentration was limited substrate ubiquitylation detected (Fig. 1e).

RNF4 has a similar mode of dimerization as the RING domains of cIAP2 (ref. 18), MDM2–MDMX¹⁹, and the U-box domain of Prp19 (ref. 20). The structure of cIAP2 was also solved in complex with E2 enzyme UbCH5b¹⁸. As RNF4 is active with UbCH5 family of E2s¹³ and several E2-interacting residues are conserved between cIAP2 and RNF4, we used the cIAP2–UbCH5b structure to model the interaction between RNF4 and UbCH5b (Fig. 1f). To verify the model, we changed putative E2-interacting residues to alanine in full-length RNF4 (Fig. 1f). With the exception of RNF4 I138A, the mutant proteins were correctly folded (Supplementary Fig. 5). Compared with wild-type RNF4, all mutations of putative E2-interacting residues reduced substrate ubiquitylation activity of RNF4 and a double mutant M140A R181A showed no detectable E3 ligase activity (Fig. 1g).

To assess dimerization, we used fluorescence resonance energy transfer (FRET). When ECFP-RNF4 was mixed with YFP-RING domain, a FRET signal was detected that leveled off within the first 20 seconds (Fig. 1h). FRET was not observed when either YFP alone or dimerization-defective mutant YFP-RING I194A was added to ECFP-RNF4. A mutant with disrupted E2-binding site (RING M140A R181A) shows a similar, but slightly reduced FRET signal. Thus, full-length RNF4 can form ‘heterodimers’ with the isolated RING domain. The rapid equilibration suggests that individual RNF4 molecules dynamically exchange between dimeric and monomeric states.

Ubiquitylation by RNF4 can proceed *in cis* and *in trans*

Dimerization is essential for ubiquitin E3 ligase activity of RNF4 and other dimeric RING domain E3s^{18,19,21}. However, monomeric RNF4 is capable of binding both substrate and E2. This poses a question, why is dimerization critical? We hypothesized that ubiquitylation would proceed *in trans*, with E2 bound to one RING monomer and substrate bound to the other. To test this, we combined mutant RNF4 with disrupted E2-binding site (RNF4 M140A R181A) and isolated RING domain of wild-type RNF4 (RING WT). Inactive RNF4 M140A R181A possesses a substrate-binding site but does not interact with E2, whereas the isolated RING domain interacts with E2 but lacks a substrate-binding site. These proteins form ‘heterodimers’ (Fig. 1h) that contain one substrate and one E2-binding site, located in different monomers, therefore ubiquitylation can proceed only *in trans*. When both RNF4 M140A R181A and RING WT were mixed, substantial substrate ubiquitylation was observed, whereas neither protein alone could efficiently ubiquitylate substrate (Fig. 2a,b). Substrate ubiquitylation activity of dimerization-deficient RNF4 I194A could not be rescued by addition of RING WT, confirming that a functional dimer is required for ubiquitylation activity of RNF4.

Ubiquitylation by RNF4 can proceed *in trans*, but is this an obligate requirement, or can the reaction also proceed *in cis*? To address this question, we titrated the RING domain with disrupted E2-binding site (RING M140A R181A) into a substrate ubiquitylation reaction containing full-length wild-type RNF4 (RNF4 WT). If ubiquitylation by RNF4 must proceed *in trans*, then heterodimers of RNF4 WT and RING M140A R181A should not possess substrate ubiquitylation activity. Therefore, addition of an excess of RING M140A R181A to wild-type RNF4 should result in inhibition of E3 ligase activity (Fig. 2c). However, addition of up to a 200 times molar excess of RING M140A R181A lead to an increase in substrate ubiquitylation activity of wild-type RNF4, rather than a decrease (Fig. 2d). Under the conditions used, substrate ubiquitylation activity was proportional to concentration of RNF4 in the reaction (Fig. 2e). As expected, RING M140A R181A efficiently formed dimers with full-length RNF4 (Supplementary Fig. 6). As the heterodimer (RNF4 WT : RING M140A R181A) is active, this suggests that ubiquitylation can proceed *in cis*. Thus, RNF4-mediated ubiquitylation can proceed both *in cis* and *in trans*, implying that dimerization, although required for ubiquitylation activity, does not impose or create a particular spatial orientation of substrate- and E2-binding sites.

RNF4 preferentially binds and activates ubiquitin-loaded E2

To gain insight into the mechanism of RING catalyzed ubiquitylation, it would be desirable to interrogate a complex between the RING domain of RNF4 and UbcH5~Ub thioester. However, in the presence of RNF4 ubiquitin undergoes rapid transfer from E2 to lysine residues on the E3 in an autoubiquitylation reaction, precluding direct study. We thus changed the active site cysteine of UbcH5a to serine such that a more stable E2~Ub oxyester could be formed. In the absence of an E3, the UbcH5a (C85S)~Ub oxyester was stable, but after addition of RNF4 the oxyester underwent hydrolysis (Fig. 3a). The isolated RING domain of RNF4 was as efficient as the full-length protein in hydrolyzing the oxyester (Fig. 3b). The oxyester-linked ubiquitin was not transferred to lysine residues in RNF4 and formation of ubiquitin chains was not detected. Mass spectrometric analysis showed that a mixture of free ubiquitin (a product of hydrolysis) and ubiquitin linked to an amine group of a Tris molecule from the reaction buffer was released from the UbcH5a (C85S)~Ub oxyester following incubation with RNF4 (Supplementary Fig. 7). The oxyester was also cleaved by RNF4 in buffers lacking primary amine groups (MOPS and HEPES).

These results indicate that binding of the UbcH5a (C85S)~Ub oxyester to the RING domain of RNF4 activates the oxyester bond between ubiquitin and E2. We therefore asked whether dimerization of the RING domain plays a role in the activation of the oxyester bond. Compared to wild-type RNF4, all the dimerization mutants were inefficient in hydrolyzing the UbcH5a (C85S)~Ub oxyester (Fig. 3b). Thus, the ability of the mutant proteins to cleave the UbcH5a (C85S)~Ub oxyester closely correlated with their substrate ubiquitylation activities. Moreover, this assay uncouples RING-mediated activation of the bond connecting E2 and ubiquitin from transfer of ubiquitin to lysines.

Since neither the UbcH5a~Ub thioester nor the UbcH5a (C85S)~Ub oxyester is stable in the presence of RNF4, we generated a double mutant UbcH5a N77A C85S with the aim of producing a stable linkage between UbcH5a and ubiquitin. Asn77 is thought to stabilize the oxyanion intermediate formed when a lysine residue from substrate attacks the E2~Ub thioester bond²². Indeed, UbcH5a (N77A C85S)~Ub was stable both in the absence and presence of RNF4 (Supplementary Fig. 8a). A mixture of UbcH5a (N77A C85S), free ubiquitin, and the E2~Ub oxyester was incubated with MBP-tagged RNF4 and bound proteins collected on amylose beads. Ubiquitin-charged UbcH5a was preferentially bound by RNF4 (Fig. 3c). Free UbcH5a interacted weakly while binding of free ubiquitin could not be detected. Monomeric mutants of RNF4 (I192A and I194A) did not show this preferential

binding of E2~Ub, nor was any interaction observed with the E2-binding deficient RNF4 M140A R181A.

Given that the UbcH5a-ubiquitin oxyester preferentially binds RNF4, the RING domain could have an additional interaction site for ubiquitin. Thus, the strict requirement for RING dimerization could be a consequence of UbcH5a binding to one monomer while the linked ubiquitin binds to the other monomer of RNF4. We positioned the UbcH5-ubiquitin thioester onto the RING domain of RNF4, using the structure of UbcH5b bound to the RING of cIAP2 (ref. 18) to position the E2 on RNF4. A structure of the E2~Ub thioester was based on the structure of the UbcH5b-ubiquitin oxyester²³. The model was generated manually by changing the position of ubiquitin relative to the E2, while retaining the thioester linkage. It is feasible to place ubiquitin across the dimer interface of the RING domain. This positions the E2 on one monomer in RNF4 while the linked ubiquitin reaches across the molecule and binds to residues in the other monomer located at the dimer interface (Fig. 3d). In this model the planar ring of Tyr193 of RNF4 engages the “Ile44 hydrophobic patch” of ubiquitin composed of Leu8, Val70 and centered on Ile44. There are also potential contacts between the side chain of Leu152 of RNF4 and ubiquitin (Fig. 3e).

“Ile44 patch” of ubiquitin is required for RNF4 activity

Most ubiquitin-binding domains interact with a solvent exposed hydrophobic patch in ubiquitin that is centered on Ile44 and includes Leu8 and Val70²⁴. Our model predicted this same surface was involved in recognition of the RNF4 RING domain. To test this, we used ubiquitin molecules in which the “hydrophobic patch” interface was altered by mutagenesis (L8A, I44A and V70A). All ubiquitin mutants were efficiently loaded as thioesters onto UbcH5a (Fig. 4a). However, L8A and I44A were inactive in substrate ubiquitylation (200-times reduced reaction rate compared to wild-type ubiquitin), while V70A showed reduced activity (Fig. 4b). Mutation of other interaction sites on ubiquitin (F4A and D58A)²⁵⁻²⁷ had no effect on substrate ubiquitylation. The intrinsic ability of UbcH5a charged with I44A ubiquitin to transfer the I44A ubiquitin to poly-L-lysine in the absence of an E3 (ref. 28) was reduced 3-times (Fig. 4c). However, this reduction in activity was small compared to the 200-times difference in E3-dependent ubiquitylation activity. The oxyester bond between ubiquitin I44A and UbcH5a C85S was completely resistant to RNF4-mediated hydrolysis (Fig. 4d) and the conjugate between UbcH5a C85S and ubiquitin I44A did not interact with RNF4 (Fig. 4e). As expected, mutation of the E2-binding site in RNF4 (M140A R181A) abrogated binding to ubiquitin-loaded E2 (Fig. 4e). It should be noted that under the conditions used binding of free E2 to RNF4 was not detected. Free E2 “pulled down” by wild-type RNF4 is a product of RNF4-mediated hydrolysis of the UbcH5a (C85S)~Ub oxyester (Supplementary Fig. 8b).

Thus, the “Ile44 hydrophobic patch” on ubiquitin is required for RNF4-mediated catalysis. However, this region also forms a noncovalent interaction with UbcH5 that influences processivity of ubiquitin addition^{23,29}. This interaction was abolished by an S22R mutation in UbcH5 (ref. 29). Although substrate ubiquitylation with UbcH5a S22R was somewhat reduced, binding of UbcH5a (S22R C85S)~Ub oxyester to RNF4 and RNF4-induced hydrolysis of the oxyester were similar to wild-type (data not shown). Thus, the loss of activity seen with the “Ile44 patch” mutants of ubiquitin is not due to disruption of the noncovalent interaction between UbcH5a and ubiquitin.

Role of Tyr193 of RNF4 in E3 ligase activity

In the model of RNF4 bound to UbcH5 loaded with ubiquitin, the E2 binds to one monomer and ubiquitin reaches across the dimer with the “Ile44 hydrophobic patch” engaging Tyr193 of the other RNF4 monomer (Fig. 3d,e). Tyr193 is required for dimerization as the Y193A

mutant is monomeric (Supplementary Fig. 5) and inactive as an E3 ligase (Fig. 1e). However, this residue is not buried in the dimer interface, but is surface exposed and appears to function by shielding the dimer interface (Fig. 1d). We therefore changed Tyr193 to histidine, reasoning that this would retain the shielding function but as the side-chain of histidine is hydrophilic rather than hydrophobic, would be unable to interact with the hydrophobic patch on ubiquitin. RNF4 Y193H (and Y193W) retained ability to dimerize, as assessed by gel filtration chromatography, and its addition to a mixture of YFP-RING domain and ECFP-RNF4 led to a reduction in FRET signal. In contrast, monomeric RNF4 Y193A was unable to effect the reduction in FRET (Fig. 5a). As expected, the monomeric mutants were inactive in single-turnover substrate ubiquitylation reactions. Y193H, although dimeric, was inactive, whereas Y193W (which retains hydrophobic character) displayed only a moderate reduction in ubiquitylation activity (Fig. 5b). Mutation of Leu152 in RNF4 (L152A is also dimeric), that appeared to contact ubiquitin in our model, showed a modest reduction in ubiquitylation activity (Fig. 5b). RNF4 Y193H was unable to efficiently catalyze hydrolysis of the UbcH5a (C85S)~Ub oxyester (Fig. 5c). Neither RNF4 Y193A nor Y193H bound UbcH5a~ubiquitin (Fig. 5d). To rescue its ubiquitylation activity, the Y193H mutant of RNF4 was mixed with a mutant with disrupted E2-binding site (RNF4 M140A R181A). Although the individual molecules were inactive, the heterodimer showed significant substrate ubiquitylation activity (Fig. 5e). We infer that in the heterodimer, the E2 component of the E2~ubiquitin thioester binds to the Y193H subunit, while the ubiquitin component of the E2~ubiquitin thioester engages Tyr193 of the M140A R181A subunit of RNF4, recreating a functional ubiquitin E3 ligase.

As the RNF4 RING is in dynamic equilibrium between monomer and dimer and only the dimer is active, the concentration of dimer is critical to evaluate the activity of RNF4. The homodimeric nature of RNF4 also means that it is not possible to introduce mutations into only one subunit of the dimer. To overcome these problems, we used a strategy previously employed for BRCA1–BARD1 (ref. 30) in which the two monomers are fused into a single polypeptide. The RNF4 RING crystal structure reveals that the C-terminus of one RING is close to the N-terminus of the other RING (Fig. 1c). We therefore fused the C-terminus of full-length RNF4 to residue 131 at the N-terminus of the RING domain to create the fusion protein containing a single substrate binding site at the N-terminus and two RING domains linked via a short spacer (Fig. 6a). Thus, mutations in the E2-binding site and Tyr193 can be asymmetrically introduced into the fusion protein. Consistent with our model, mutation of the E2-binding site (M140A R181A) in only one RING did not affect substrate ubiquitylation activity (Fig. 6b). Likewise, introduction of the Y193A mutation into one RING was without consequence. However, introduction of the E2-binding site mutations or the Y193A mutation into both RINGs dramatically reduced ubiquitylation activity (Fig. 6b). Combining the E2-binding site mutations with the Y193A mutation in the same RING abrogated E3 ligase activity, whereas introducing the E2-binding site mutations into one RING and the Y193A mutation into the other RING gave wild-type activity (Fig. 6b). These data confirm the requirement for E2-binding site and Tyr193 to be present on opposite subunits of the RNF4 dimer.

To establish the role of Tyr193 in ubiquitin transfer, we carried out Michaelis-Menten analysis of substrate ubiquitylation comparing the fusion proteins where E2-binding site and Y193A mutations are in the same RING or in different RINGs. With $4 \times$ SUMO-2 substrate in excess, initial rate measurements of substrate ubiquitylation were collected at a range of concentrations of ubiquitin-loaded E2. The RNF4-RING fusion with E2-binding site and Y193A mutations in different RINGs, that displays wild-type activity, has a K_M for ubiquitin-loaded UbcH5a that is 8-times lower and a v_{max} that is 10-times higher than the otherwise identical fusion that has the E2-binding site and Y193A mutations in the same RING (Fig. 6c). This suggests that ubiquitin-loaded E2 has a higher affinity for the RING

dimer when it can engage the Tyr193 residue from the RING subunit that does not interact with E2. However, the data also indicate that engagement of Tyr193 in the RING by ubiquitin-loaded E2 has a direct effect on catalysis. Consistent with the effect on K_M , the RNF4-RING fusion proteins with E2-binding site and Y193A mutations in the same RING did not efficiently bind ubiquitin-loaded E2, while versions of RNF4-RING with these mutations in opposite RINGs displayed selective binding of ubiquitin-loaded E2 (Fig. 6d).

Discussion

Dimeric RING ubiquitin ligases are modular proteins containing a substrate-binding domain and a RING domain that is the catalytic engine of ubiquitylation. This is exemplified by RNF4 where its N-terminal domain binds to the poly-SUMO substrate, while the RING domain is responsible for ubiquitin transfer. RING dimerization is essential for ubiquitin E3 ligase activity of RNF4, but a mechanistic understanding of this requirement has remained elusive¹⁷. Modelling suggested that UbcH5 could bind to one monomer of RNF4 while the thioester-linked ubiquitin reached across the molecule to contact the other monomer of the dimer. In this model the “hydrophobic patch” centred on Ile44 of ubiquitin engaged conserved Tyr193 located at the dimer interface. Mutation of residues in the “hydrophobic patch” of ubiquitin abrogated RING dependent transfer of ubiquitin to substrate, preferential binding of ubiquitin-loaded E2 to the RING, and RING dependent activation of the E2~ubiquitin bond. RNF4 Y193H, although dimeric, was inactive and unable to preferentially bind ubiquitin-loaded UbcH5a, consistent with the requirement for a hydrophobic residue to engage the “Ile44 patch”. The other critical interface was between UbcH5a and the RING: mutations in the RING that disrupted this interaction resulted in an inactive E3 ligase and abolished binding of ubiquitin-loaded E2.

Creation of a fusion between the two RINGs of RNF4 allowed us to directly test the requirement for the E2-binding site and Tyr193 within the context of the dimer. Mutating these sites in the same RING dramatically reduced ubiquitylation, while a dimer with these mutations in opposite RINGs had wild-type activity. Michaelis-Menten analysis of these mutants revealed that the decreased activity was due to an increased K_M for ubiquitin-loaded E2 and a decreased v_{max} for ubiquitin transfer to substrate. These data, together with our direct binding data, suggest that an E2-binding site in one RING and Tyr193 in the other RING are both required to recruit the ubiquitin-loaded E2. Presumably, this interaction alters the conformation of the active site of the E2, facilitating ubiquitin transfer to a lysine residue in substrate. This is consistent with our data which indicate that binding of both E2 and ubiquitin to RNF4 causes activation of the thioester bond in E2~Ub. Once isopeptide bond formation has taken place, the weak binding of free E2 and ubiquitin would favor their dissociation and facilitate rapid rebinding of ubiquitin-charged E2 required for processive synthesis of ubiquitin chains^{31,32}.

Homo- or heterodimerization was observed for a number of RING-type ubiquitin E3 ligases, including cIAP2 (ref. 18), TRAF6 (ref. 21), MDM2-MDMX¹⁹, BRCA1-BARD1 (ref. 33), and Ring1b-Bmi1 (ref. 34), and also for structurally related U-box ubiquitin E3 ligases Prp19 (ref. 20) and CHIP^{35,36}. Even though structural elements that form dimerization interfaces in these dimers vary, relative orientation of the two RING or U-box domains is similar. As dimerization is necessary for ubiquitylation activity, this suggests similar catalytic mechanism for these dimeric ubiquitin E3 ligases.

Our results indicate that the RING domain of RNF4 contacts both E2 and ubiquitin upon binding to the E2~Ub thioester. A similar finding was recently reported for the HECT-type ubiquitin E3 ligase NEDD4L, where a structure with UbcH5b~Ub revealed that extensive noncovalent interactions between ubiquitin and the HECT domain were required for proper

positioning of E2 and E3 active sites³⁷. An interesting interaction was also observed between UbcH5~Ub and SspH2, an atypical bacterial ubiquitin E3 ligase³⁸. SspH2 had no detectable affinity for free UbcH5, but bound to ubiquitin-charged UbcH5, recognizing regions on both E2 and ubiquitin³⁸. Although these E3 ligases are mechanistically very different, noncovalent interactions between ubiquitin and E3 might be a common theme in E3-catalyzed ubiquitylation reactions.

In our model the ubiquitin linked to the E2 is in an extended conformation that is based on the structure of a UbcH5b~ubiquitin oxyster²³ where the “Ile44 hydrophobic patch” of ubiquitin engages in a “backside” interaction with UbcH5b. While this “backside” interaction may be important for processive ubiquitin addition, it is not required for substrate ubiquitylation mediated by RNF4 as an S22R mutation in UbcH5a had a much smaller effect on substrate ubiquitylation than mutations of the “Ile44 patch” in ubiquitin. Even in the absence of this “backside” interaction the UbcH5a~ubiquitin is likely to be in an extended conformation as this was observed by NMR for the UbcH5c (S22R C85S)~ubiquitin conjugate³⁹. Recent studies on K11 chain synthesis by Ube2S have suggested that the donor ubiquitin also makes noncovalent contacts with the E2 to which it is thioester-linked via the “Ile44 hydrophobic patch”⁴⁰. This interaction was also shown to be important for the ability of ubiquitin to act as a donor for chain initiation or elongation by ubiquitin-loaded Cdc34 (ref. 41). While I44A ubiquitin had a reduced inherent ability to be transferred from E2 to substrate in the absence of an E3 (Fig. 4c), this effect was rather modest (3-times reduced) and is unlikely to account for the large (200-times reduced) E3-dependent effect we observed with this mutant (Fig. 4b).

RING domain ubiquitin E3 ligases are often viewed as scaffold proteins that bring ubiquitin-charged E2 and a substrate into close proximity and thus facilitate transfer of ubiquitin from E2 to the substrate. However, our data indicate that dimeric RING-type ubiquitin E3 ligases play a more active role, facilitating catalysis by binding both E2 and ubiquitin and thus activating the E2~Ub thioester bond.

Methods

cDNA constructs

Constructs for full-length *Rattus norvegicus* RNF4 (wild-type RNF4) and RNF4 mtSIM1,2,3,4 (SIMs mutant) were described previously¹³. The RING domain of RNF4 (residues 134–194), RNF4 32–76 (residues 32–76) and RNF4 32–133 (residues 32–133) were sub-cloned into pLou3 vector¹³ and as a result of cloning, these constructs contain three extra residues (Gly-Ala-Met) after the TEV protease cleavage site. RNF4 Δ C (residues 1–190) in pLou3 vector was a kind gift from Dr. Linnan Shen, University of Dundee. To generate a linear fusion of full-length RNF4 and the RING domain of RNF4 (termed RNF4-RING), full-length RNF4 was sub-cloned into pLou3 vector using NcoI and BamHI restriction sites, while the RNF4 RING domain (residues 131–194) was inserted using BamHI and HindIII sites. There is a single glycine residue as a linker between RNF4 and the RNF4 RING domain. For FRET-based assays, RNF4 and the RING domain of RNF4 were sub-cloned into pHIS-TEV-ECFP and pHIS-TEV-Venus-YFP plasmids⁴². 4 \times SUMO-2, a linear head-to-tail fusion of four SUMO-2 molecules, was sub-cloned into pHIS-TEV-30a vector⁴³. All SUMO-2s in the fusion protein have the first methionine changed to glycine. Details of cloning are available upon request. Human UbcH5a was sub-cloned into pHIS-TEV-30a vector. Point mutations were introduced using QuikChange site-directed mutagenesis kit (Stratagene).

Protein expression and purification

Proteins were expressed in bacteria and purified by standard methods. Detailed protocols are in Supplementary Methods.

Crystallization and structure determination

Crystals of the RING domain of RNF4 were grown using the sitting drop vapor diffusion method at 20°C. 1 μ l of the RNF4 RING domain (5.5 mg ml⁻¹ in 20 mM Tris, 150 mM NaCl, 1 mM TCEP, pH 7.0) was mixed with 1 μ l of reservoir solution (2M (NH₄)₂SO₄, 200 mM NaCl, 100 mM sodium cacodylate pH 7.0) and 0.2 μ l of 30% (w/v) sucrose. Crystals grew to their final size of ~0.15 \times 0.15 \times 0.15 mm in 2–3 days. Before flash-freezing in liquid nitrogen, crystals were briefly soaked in a cryoprotectant solution (15:85 (v/v) reservoir solution and saturated solution of sucrose in the reservoir solution).

Diffraction data were collected at 100 K at beamline ID14-4 at the European Synchrotron Radiation Facility, Grenoble, France. The structure was solved by SAD using the anomalous signal from the two zinc ions bound to the RING domain. A SAD data set was collected at the zinc absorption peak wavelength (1.28 Å, determined by fluorescence scan). A second data set for refinement from a different crystal was collected at a wavelength of 0.98 Å. All diffraction data were processed using HKL2000 (ref. 44). Phases were obtained using SHELXC/D/E⁴⁵ and an initial model was built by ARP/wARP⁴⁶. This model was refined using REFMAC5 (ref. 47) from the CCP4 suite⁴⁸, followed by iterative cycles of manual rebuilding using Coot⁴⁹ and further refinement. Translation, libration and screw rotation (TLS) parameters were used in the final cycles of refinement⁵⁰. Data collection and refinement statistics are shown in Table 1. The geometry of the final model was checked with MolProbity⁵¹. 98.4% of residues were found to be in the favored region of the Ramachandran plot, with the remaining 1.6% being in the allowed region. The dimerization interface of RNF4 was analyzed using the PISA server at the European Bioinformatics Institute⁵². Structural representations and models were generated using PyMol (Schrödinger).

Single-turnover substrate ubiquitylation assay

E2 (UbcH5a) was first charged with ubiquitin in the absence of an E3 and a substrate. To prepare the UbcH5a~Ub thioester, UbcH5a and ubiquitin (both 100 μ M) were incubated with 0.2 μ M Ube1 in 50 mM Tris, 150 mM NaCl, 3 mM ATP, 5 mM MgCl₂, 0.5 mM TCEP, 0.1% (v/v) NP40, pH 7.5 at 37°C for 12 min. To stop E1-mediated loading of E2 with ubiquitin, ATP was depleted by addition of apyrase (4.5 U ml⁻¹; New England BioLabs) and the reaction was incubated at room temperature for 10 min. Efficiency of UbcH5a~Ub thioester formation was estimated to be approximately 60%. ¹²⁵I-labeled 4 \times SUMO-2 (~750 Ci mol⁻¹) was used as a substrate for RNF4-mediated ubiquitylation. The UbcH5a~Ub thioester (~20 μ M) was incubated with RNF4 (0.275 μ M unless specified otherwise in the figure legend) and ¹²⁵I-4 \times SUMO-2 (5.5 μ M) at room temperature. Reactions were stopped by addition of reducing SDS-PAGE loading buffer and analyzed by SDS-PAGE followed by phosphorimaging. Percentage of substrate modified with ubiquitin was determined by quantification of phosphorimager scans using AIDA software (Raytest). Reaction time points were taken from 30 seconds to up to 20 minutes and reaction rates were determined using at least three time points within the linear range of the reaction. Reactions were carried out in duplicate and reaction rates are shown as mean \pm standard deviation. Examples of primary data are shown in Supplementary Fig. 9.

Substrate ubiquitylation reactions with RNF4-RING linear fusion proteins as E3 contained ~20 μ M UbcH5a~Ub thioester, 5.5 μ M ¹²⁵I-4 \times SUMO-2, and 35 nM RNF4-RING fusion protein. To determine Michaelis-Menten kinetics, initial rate measurements of substrate

ubiquitylation were collected at a range of concentrations of the Ub_{H5a}-Ub thioester (0.5 μ M – 60 μ M). Reaction time points were taken from 1 minute to up to 4 minutes for RNF4 (M140A R181A)-RING (Y193A), and from 15 minutes to up to 2 hours for RNF4 (M140A R181A Y193A)-RING (WT). Reaction rates were determined using three time points within the linear range of the reaction. Data were analyzed using GraphPad Prism (GraphPad Software).

Other biochemical assays

Detailed procedures are described in Supplementary Methods.

Supplementary Material

Refer to Web version on PubMed Central for supplementary material.

Acknowledgments

We would like to thank Catherine Botting (University of St. Andrews) for mass spectrometric analysis, Mark Agacan (University of Dundee) for analytical ultracentrifugation analysis and Nicola Wood (University of Dundee) for help with cloning. His-Ube1 was a kind gift from the Division of Signal Transduction Therapy, University of Dundee. A.P. was funded by a studentship from the Wellcome Trust. This work was supported by a grant to R.T.H. from Cancer Research UK. The structural biology was supported by the Scottish Funding Council (reference SULSA) and by the BBSRC through the SPoRT initiative.

References

1. Dye BT, Schulman BA. Structural mechanisms underlying posttranslational modification by ubiquitin-like proteins. *Annu. Rev. Biophys. Biomol. Struct.* 2007; 36:131–150. [PubMed: 17477837]
2. Pickart CM, Eddins MJ. Ubiquitin: structures, functions, mechanisms. *Biochim. Biophys. Acta.* 2004; 1695:55–72. [PubMed: 15571809]
3. Deshaies RJ, Joazeiro CA. RING domain E3 ubiquitin ligases. *Annu. Rev. Biochem.* 2009; 78:399–434. [PubMed: 19489725]
4. Hay RT. SUMO: a history of modification. *Mol. Cell.* 2005; 18:1–12. [PubMed: 15808504]
5. Perry JJ, Tainer JA, Boddy MN. A SIM-ultaneous role for SUMO and ubiquitin. *Trends Biochem. Sci.* 2008; 33:201–208. [PubMed: 18403209]
6. Kosoy A, Calonge TM, Outwin EA, O'Connell MJ. Fission yeast Rnf4 homologs are required for DNA repair. *J. Biol. Chem.* 2007; 282:20388–20394. [PubMed: 17502373]
7. Prudden J, et al. SUMO-targeted ubiquitin ligases in genome stability. *EMBO J.* 2007; 26:4089–40101. [PubMed: 17762865]
8. Sun H, Levenson JD, Hunter T. Conserved function of RNF4 family proteins in eukaryotes: targeting a ubiquitin ligase to SUMOylated proteins. *EMBO J.* 2007; 26:4102–4112. [PubMed: 17762864]
9. Uzunova K, et al. Ubiquitin-dependent proteolytic control of SUMO conjugates. *J. Biol. Chem.* 2007; 282:34167–34175. [PubMed: 17728242]
10. Xie Y, et al. The yeast Hex3.Slx8 heterodimer is a ubiquitin ligase stimulated by substrate sumoylation. *J. Biol. Chem.* 2007; 282:34176–34184. [PubMed: 17848550]
11. Hakli M, Lorick KL, Weissman AM, Janne OA, Palvimo JJ. Transcriptional coregulator SNURF (RNF4) possesses ubiquitin E3 ligase activity. *FEBS Lett.* 2004; 560:56–62. [PubMed: 14987998]
12. Lallemand-Breitenbach V, et al. Arsenic degrades PML or PML-RAR α through a SUMO-triggered RNF4/ubiquitin-mediated pathway. *Nat. Cell Biol.* 2008; 10:547–555. [PubMed: 18408733]
13. Tatham MH, et al. RNF4 is a poly-SUMO-specific E3 ubiquitin ligase required for arsenic-induced PML degradation. *Nat. Cell Biol.* 2008; 10:538–546. [PubMed: 18408734]

14. Song J, Durrin LK, Wilkinson TA, Krontiris TG, Chen Y. Identification of a SUMO-binding motif that recognizes SUMO-modified proteins. *Proc. Natl. Acad. Sci. USA*. 2004; 101:14373–14378. [PubMed: 15388847]
15. Hecker CM, Rabiller M, Haglund K, Bayer P, Dikic I. Specification of SUMO1- and SUMO2-interacting motifs. *J. Biol. Chem.* 2006; 281:16117–16127. [PubMed: 16524884]
16. Song J, Zhang Z, Hu W, Chen Y. Small ubiquitin-like modifier (SUMO) recognition of a SUMO binding motif: a reversal of the bound orientation. *J. Biol. Chem.* 2005; 280:40122–40129. [PubMed: 16204249]
17. Liew CW, Sun H, Hunter T, Day CL. RING domain dimerization is essential for RNF4 function. *Biochem. J.* 2010; 431:23–29. [PubMed: 20681948]
18. Mace PD, et al. Structures of the cIAP2 RING domain reveal conformational changes associated with ubiquitin-conjugating enzyme (E2) recruitment. *J. Biol. Chem.* 2008; 283:31633–31640. [PubMed: 18784070]
19. Linke K, et al. Structure of the MDM2/MDMX RING domain heterodimer reveals dimerization is required for their ubiquitylation in trans. *Cell Death Differ.* 2008; 15:841–848. [PubMed: 18219319]
20. Vander Kooi CW, et al. The Prp19 U-box crystal structure suggests a common dimeric architecture for a class of oligomeric E3 ubiquitin ligases. *Biochemistry.* 2006; 45:121–130. [PubMed: 16388587]
21. Yin Q, et al. E2 interaction and dimerization in the crystal structure of TRAF6. *Nat. Struct. Mol. Biol.* 2009; 16:658–666. [PubMed: 19465916]
22. Wu PY, et al. A conserved catalytic residue in the ubiquitin-conjugating enzyme family. *EMBO J.* 2003; 22:5241–5250. [PubMed: 14517261]
23. Sakata E, et al. Crystal structure of UbcH5b-ubiquitin intermediate: insight into the formation of the self-assembled E2-Ub conjugates. *Structure.* 2010; 18:138–147. [PubMed: 20152160]
24. Dikic I, Wakatsuki S, Walters KJ. Ubiquitin-binding domains - from structures to functions. *Nat. Rev. Mol. Cell Biol.* 2009; 10:659–671. [PubMed: 19773779]
25. Lee S, et al. Structural basis for ubiquitin recognition and autoubiquitination by Rabex-5. *Nat. Struct. Mol. Biol.* 2006; 13:264–271. [PubMed: 16462746]
26. Penengo L, et al. Crystal structure of the ubiquitin binding domains of rabex-5 reveals two modes of interaction with ubiquitin. *Cell.* 2006; 124:1183–1195. [PubMed: 16499958]
27. Rahighi S, et al. Specific recognition of linear ubiquitin chains by NEMO is important for NF- κ B activation. *Cell.* 2009; 136:1098–1109. [PubMed: 19303852]
28. Mastrandrea LD, Kasperek EM, Niles EG, Pickart CM. Core domain mutation (S86Y) selectively inactivates polyubiquitin chain synthesis catalyzed by E2-25K. *Biochemistry.* 1998; 37:9784–9792. [PubMed: 9657692]
29. Brzovic PS, Lissounov A, Christensen DE, Hoyt DW, Kleivit RE. A UbcH5/ubiquitin noncovalent complex is required for processive BRCA1-directed ubiquitination. *Mol. Cell.* 2006; 21:873–880. [PubMed: 16543155]
30. Christensen DE, Brzovic PS, Kleivit RE. E2-BRCA1 RING interactions dictate synthesis of mono- or specific polyubiquitin chain linkages. *Nat. Struct. Mol. Biol.* 2007; 14:941–948. [PubMed: 17873885]
31. Kleiger G, Saha A, Lewis S, Kuhlman B, Deshaies RJ. Rapid E2-E3 assembly and disassembly enable processive ubiquitylation of cullin-RING ubiquitin ligase substrates. *Cell.* 2009; 139:957–968. [PubMed: 19945379]
32. Pierce NW, Kleiger G, Shan SO, Deshaies RJ. Detection of sequential polyubiquitylation on a millisecond timescale. *Nature.* 2009; 462:615–619. [PubMed: 19956254]
33. Brzovic PS, Rajagopal P, Hoyt DW, King MC, Kleivit RE. Structure of a BRCA1-BARD1 heterodimeric RING-RING complex. *Nat. Struct. Biol.* 2001; 8:833–837. [PubMed: 11573085]
34. Buchwald G, et al. Structure and E3-ligase activity of the Ring-Ring complex of Polycomb proteins Bmi1 and Ring1b. *EMBO J.* 2006; 25:2465–2474. [PubMed: 16710298]
35. Xu Z, et al. Interactions between the quality control ubiquitin ligase CHIP and ubiquitin conjugating enzymes. *BMC Struct. Biol.* 2008; 8:26. [PubMed: 18485199]

36. Zhang M, et al. Chaperoned ubiquitylation—crystal structures of the CHIP U box E3 ubiquitin ligase and a CHIP-Ubc13-Uev1a complex. *Mol. Cell.* 2005; 20:525–538. [PubMed: 16307917]
37. Kamadurai HB, et al. Insights into ubiquitin transfer cascades from a structure of a UbcH5B~ubiquitin-HECT(NEDD4L) complex. *Mol. Cell.* 2009; 36:1095–1102. [PubMed: 20064473]
38. Levin I, et al. Identification of an unconventional E3 binding surface on the UbcH5~Ub conjugate recognized by a pathogenic bacterial E3 ligase. *Proc. Natl. Acad. Sci. USA.* 2010; 107:2848–2853. [PubMed: 20133640]
39. Pruneda JN, Stoll KE, Bolton LJ, Brzovic PS, Kleivit RE. Ubiquitin in motion: structural studies of the ubiquitin-conjugating enzyme~ubiquitin conjugate. *Biochemistry.* 2011; 50:1624–1633. [PubMed: 21226485]
40. Wickliffe KE, Lorenz S, Wemmer DE, Kuriyan J, Rape M. The mechanism of linkage-specific ubiquitin chain elongation by a single-subunit E2. *Cell.* 2011; 144:769–781. [PubMed: 21376237]
41. Saha A, Lewis S, Kleiger G, Kuhlman B, Deshaies RJ. Essential role for ubiquitin-ubiquitin-conjugating enzyme interaction in ubiquitin discharge from Cdc34 to substrate. *Mol. Cell.* 2011; 42:75–83. [PubMed: 21474069]
42. Martin SF, Tatham MH, Hay RT, Samuel ID. Quantitative analysis of multi-protein interactions using FRET: application to the SUMO pathway. *Protein Sci.* 2008; 17:777–784. [PubMed: 18359863]
43. Martin SF, Hattersley N, Samuel ID, Hay RT, Tatham MH. A fluorescence-resonance-energy-transfer-based protease activity assay and its use to monitor paralog-specific small ubiquitin-like modifier processing. *Anal. Biochem.* 2007; 363:83–90. [PubMed: 17288980]
44. Otwinowski Z, Minor W. Processing of X-ray diffraction data collected in oscillation mode. *Methods Enzymol.* 1997; 276:307–326.
45. Sheldrick GM. A short history of SHELX. *Acta Crystallogr. A.* 2008; 64:112–122. [PubMed: 18156677]
46. Morris RJ, Perrakis A, Lamzin VS. ARP/wARP and automatic interpretation of protein electron density maps. *Methods Enzymol.* 2003; 374:229–244. [PubMed: 14696376]
47. Murshudov GN, Vagin AA, Dodson EJ. Refinement of macromolecular structures by the maximum-likelihood method. *Acta Crystallogr. D Biol. Crystallogr.* 1997; 53:240–255. [PubMed: 15299926]
48. Winn MD, et al. Overview of the CCP4 suite and current developments. *Acta Crystallogr. D Biol. Crystallogr.* 2011; 67:235–242. [PubMed: 21460441]
49. Emsley P, Lohkamp B, Scott WG, Cowtan K. Features and development of Coot. *Acta Crystallogr. D Biol. Crystallogr.* 2010; 66:486–501. [PubMed: 20383002]
50. Winn MD, Isupov MN, Murshudov GN. Use of TLS parameters to model anisotropic displacements in macromolecular refinement. *Acta Crystallogr. D Biol. Crystallogr.* 2001; 57:122–133. [PubMed: 11134934]
51. Davis IW, et al. MolProbity: all-atom contacts and structure validation for proteins and nucleic acids. *Nucleic Acids Res.* 2007; 35:W375–W383. [PubMed: 17452350]
52. Krissinel E, Henrick K. Inference of macromolecular assemblies from crystalline state. *J. Mol. Biol.* 2007; 372:774–797. [PubMed: 17681537]

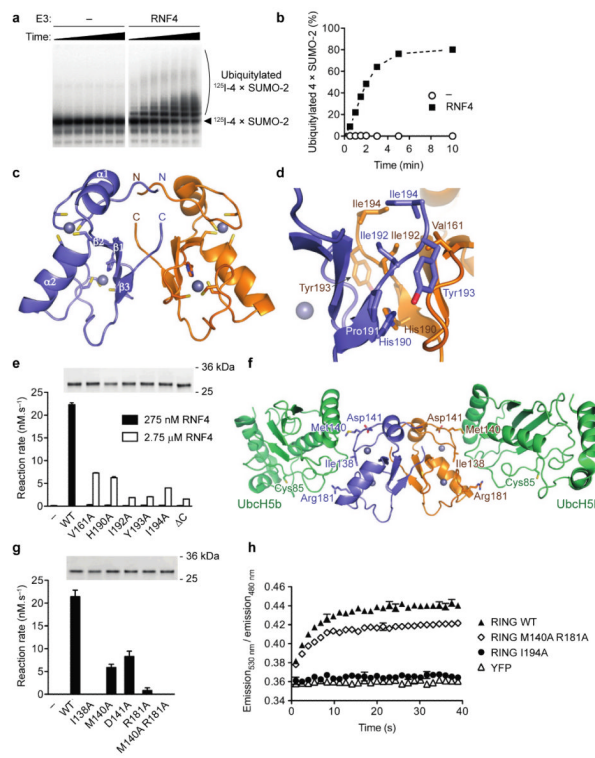
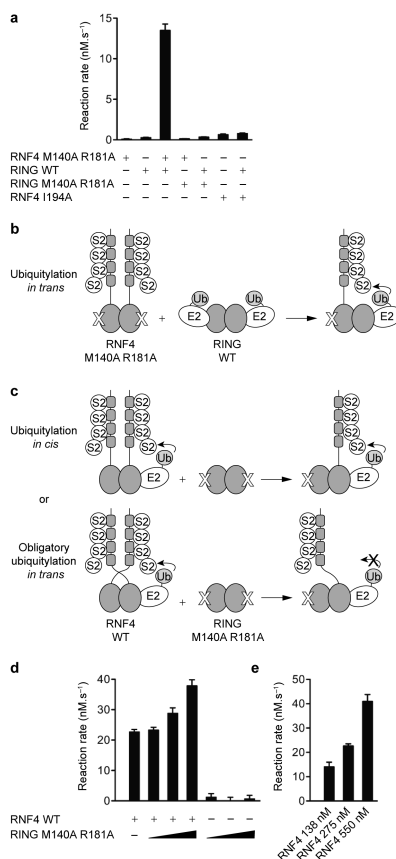
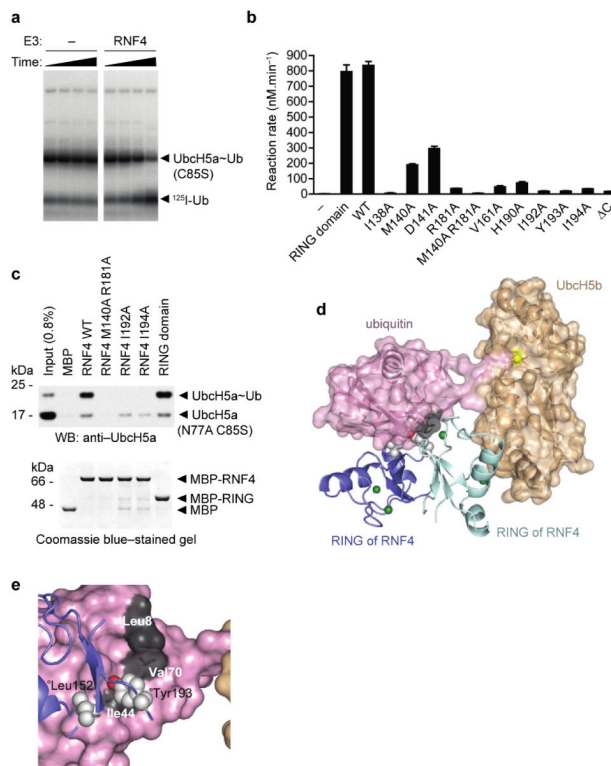


Figure 1.

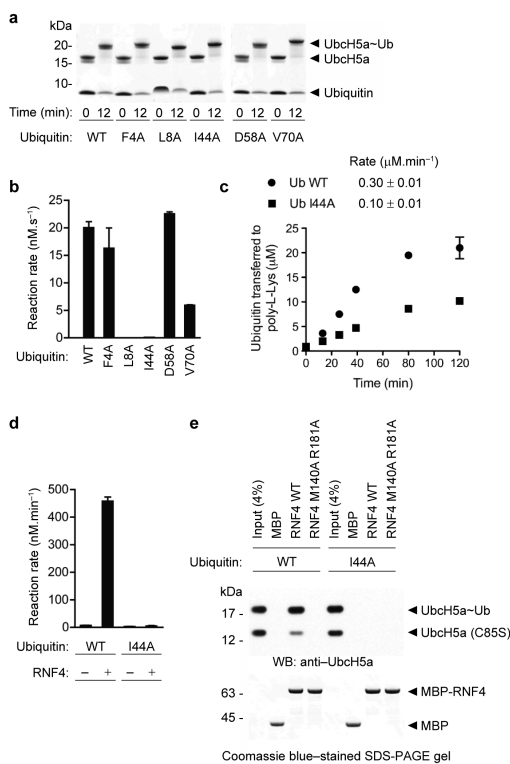
Structure of dimeric RING domain of RNF4. **(a)** Single-turnover substrate ubiquitylation assay for RNF4. The UbcH5a~Ub thioester was incubated with ^{125}I -labeled $4 \times \text{SUMO-2}$ in the presence or absence of RNF4, followed by SDS-PAGE analysis and phosphorimaging. **(b)** Quantification of substrate ubiquitylation reactions shown in **a**. **(c)** Cartoon representation of the dimer of the RNF4 RING domain. Zinc ions are shown as grey spheres and zinc co-ordinating residues in stick representation. **(d)** A close up view of the dimerization interface of RNF4. Residues at the dimer interface are shown in stick representation. Atoms are color-coded as follows: nitrogens in blue, oxygens in red and sulphurs in yellow. **(e)** Mutational analysis of dimerization interface residues. Substrate ubiquitylation activity of dimerization mutants of RNF4 was determined using the single-turnover ubiquitylation assay described in panel **a**. Data represent mean \pm s.d. of duplicate reactions. The upper panel shows a Coomassie blue-stained SDS-PAGE gel with purified wild-type (WT) and mutant RNF4 proteins ($1 \mu\text{g}$). **(f)** A model of a complex between the RNF4 RING domain and UbcH5b. Putative E2-binding residues of RNF4 that were mutated in this study are shown in stick representation. Active site cysteine of UbcH5b (Cys85) is also shown. **(g)** Substrate ubiquitylation activity of E2-binding mutants of RNF4. **(h)** A FRET-based *in vitro* assay to study dimerization of RNF4. ECFP-RNF4 (wild-type) was mixed with YFP or YFP-RING domain of RNF4 (wild-type or mutant as indicated) and FRET signal was measured. Data points represent mean \pm s.d. of triplicate measurements.

**Figure 2.**

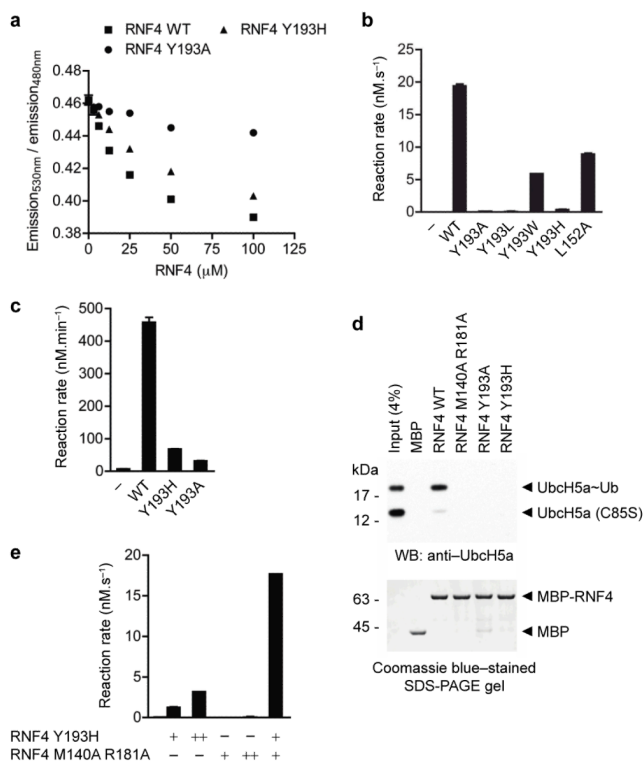
Ubiquitylation by RNF4 can proceed both *in cis* and *in trans*. **(a)** Ubiquitylation by RNF4 can proceed *in trans*. Full-length RNF4 (0.55 μM) and the RNF4 RING domain (0.55 μM) were added to substrate ubiquitylation reactions as indicated and ubiquitylation activity was determined. **(b)** Schematic representation of the experiment in **a**. A heterodimer of the RNF4 RING domain and full-length RNF4 with disrupted E2-binding site (M140A R181A) should be active in a substrate ubiquitylation reaction provided ubiquitylation by RNF4 can proceed *in trans*. S2, SUMO-2; Ub, ubiquitin. **(c)** Schematic representation of a hypothesis behind the experiment in **d**. If ubiquitylation by RNF4 can proceed *in cis*, then a heterodimer of full-length RNF4 and the RNF4 RING domain with disrupted E2-binding site should possess substrate ubiquitylation activity. However, this heterodimer should be inactive if ubiquitylation can only proceed *in trans*. Therefore, addition of an excess of the RING domain with disrupted E2-binding site to wild-type RNF4 should result in inhibition of substrate ubiquitylation activity provided ubiquitylation cannot proceed *in cis*. **(d)** Ubiquitylation by RNF4 can proceed *in cis*. The RING domain of RNF4 with disrupted E2-binding site (RING M140A R181A) was added to RNF4 WT (0.275 μM) in 2, 20, and 200-times molar excess, respectively, and substrate ubiquitylation activity was determined. **(e)** Under the conditions used in **d**, substrate ubiquitylation activity is proportional to concentration of RNF4 in the reaction. In **a**, **d**, and **e**, the data are mean ± s.d. of duplicate reactions. The experiments were performed twice.

**Figure 3.**

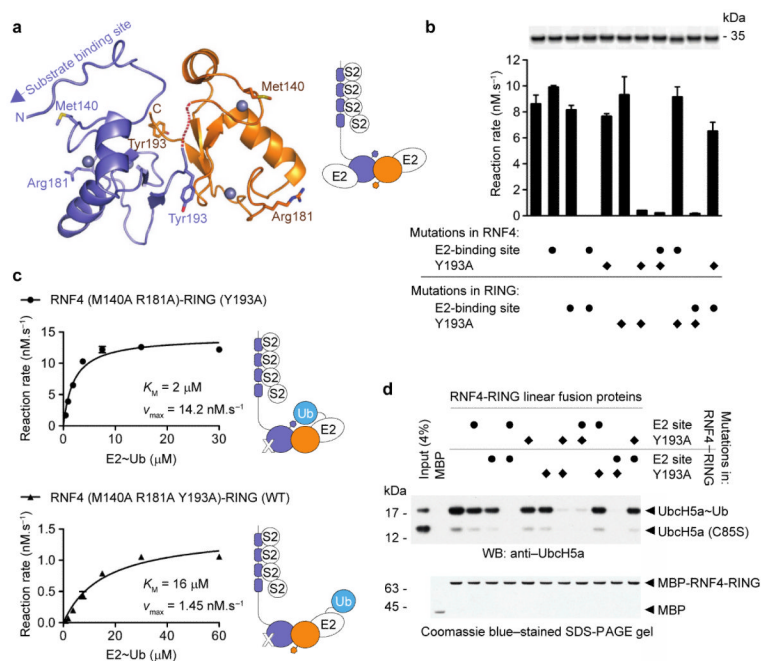
RNF4 preferentially binds ubiquitin-loaded E2 and activates the bond between E2 and ubiquitin. **(a)** RNF4 induces hydrolysis of E2~Ub linked via an oxyester bond. Phosphorimager scan of SDS-PAGE gels showing time course of Ubch5a (C85S)~¹²⁵I-Ub oxyester stability in the presence or absence of RNF4. **(b)** Ubch5a (C85S)~¹²⁵I-Ub oxyester was incubated with the RNF4 RING domain or full-length RNF4 (wild-type or mutant as indicated) and rates of oxyester hydrolysis were determined. Data are shown as mean ± s.d. of duplicate reactions. The experiment was performed two times. **(c)** RNF4 shows higher affinity for ubiquitin-charged E2 than for free E2 in a pull-down experiment. A mixture of Ubch5a (N77A C85S), ubiquitin, and the Ubch5a (N77A C85S)~Ub oxyester was incubated with MBP or MBP-RNF4 (wild-type or mutant), followed by purification on amylose beads. WB, Western blot. **(d)** A model of the RNF4 RING domain in complex with E2~ubiquitin thioester predicts an interaction between ubiquitin and the RING domain. The RING domain is shown in cartoon form, with one monomer in blue and the other monomer in cyan. Putative ubiquitin-interacting residues (Tyr193 and Leu152) are shown as spheres. Ubiquitin is shown in pink with the hydrophobic contact surface (Leu8, Ile44 and Val70) in black. The E2 is shown colored in wheat with the point of thioester attachment shown as a yellow sphere. **(e)** A close up view of the predicted interaction interface between the hydrophobic patch on ubiquitin and residues Tyr193 and Leu152 on the RING domain of RNF4.

**Figure 4.**

The “Ile44-centered hydrophobic patch” on ubiquitin is required for RNF4-mediated ubiquitylation. **(a)** Mutations in ubiquitin, used in the experiment shown in **b**, do not affect formation of the UbcH5a~Ub thioester. UbcH5a was incubated with ubiquitin in the presence of Ube1 and ATP, followed by nonreducing SDS-PAGE analysis. **(b)** Effect of mutations in ubiquitin on substrate ubiquitylation activity of RNF4. 4 × SUMO-2, radiolabeled with iodine-125, was used as substrate. Data are shown as mean ± s.d. of duplicate reactions. The experiment was performed two times. **(c)** Mutation I44A in ubiquitin causes a modest defect in E3-independent transfer of ubiquitin to poly-L-lysine. UbcH5a~¹²⁵I-Ub thioester was incubated with poly-L-lysine and time points were taken as indicated. Subsequently, poly-L-lysine was purified on SP-sepharose resin and radioactivity captured on the beads was quantified by γ -counting. Initial rates were determined from the first three time points. **(d)** The “Ile44 patch” on ubiquitin is essential for RNF4-mediated cleavage of E2~ubiquitin oxyester. The UbcH5a (C85S)~Ub oxyester was incubated in the presence or absence of RNF4 and reaction progress was analyzed by SDS-PAGE, followed by staining with SYPRO Orange. Reaction rates represent mean ± s.d. of duplicate reactions. The experiment was performed three times. **(e)** The “Ile44 patch” on ubiquitin is required for the interaction between ubiquitin-loaded E2 and RNF4. A mixture of UbcH5a (C85S), ubiquitin, and the UbcH5a (C85S)~Ub oxyester was briefly incubated with either MBP or MBP-RNF4 immobilized on amylose beads, followed by a quick washing step. Bound material was resolved by SDS-PAGE.

**Figure 5.**

Tyrosine 193, a residue located at the dimer interface of the RNF4 RING domain, is required for activation of the thioester bond in the E2~ubiquitin thioester. **(a)** The ability of RNF4 Y193H to dimerize was assessed using a FRET-based dimerization assay. Unlabeled RNF4 was titrated into a mixture of ECFP-RNF4 and YFP-RING domain and FRET signal was measured. Data points represent mean \pm s.d. of triplicate measurements. **(b)** Mutational analysis of the predicted ubiquitin-binding site on the RNF4 RING domain. Several mutations of Tyr193 were generated. Whereas mutations to alanine and leucine disrupted dimerization, mutations to tryptophan and histidine retained the ability of RNF4 to dimerize. Substrate ubiquitylation activity of the mutant proteins was determined using the single-turnover assay described in Fig. 1a. **(c)** Tyr193 in RNF4 is required for efficient hydrolysis of the E2~ubiquitin oxyester. The UbcH5a (C85S)~Ub oxyester was incubated with RNF4 (wild-type or mutant as indicated) and the rate of oxyester hydrolysis was determined. **(d)** Mutation Y193H in RNF4 disrupts binding to the E2~ubiquitin oxyester. A pull-down experiment was performed as described in Fig. 4e. **(e)** Ubiquitylation activity of RNF4 Y193H can be rescued by addition of an inactive RNF4 mutant with disrupted E2-binding site (RNF4 M140A R181A). Substrate ubiquitylation activity was determined as described in Fig. 1a. Final concentration of RNF4 mutants in the reaction was either $0.55 \mu\text{M}$ (+) or $1.1 \mu\text{M}$ (++) . In panels **b**, **c**, and **e**, data represent mean \pm s.d. of duplicate reactions. The experiments were performed two times.

**Figure 6.**

A linear fusion of full-length RNF4 and the RNF4 RING domain shows that E2-binding site in one RING domain and Tyr193 in the other RING are both required for ubiquitylation activity. **(a)** A model of a linear fusion of full-length RNF4 and the RING domain of RNF4, based on the structure of the RNF4 RING domain reported herein. A short linker between the C-terminus of full-length RNF4 and the N-terminus of the RING domain is shown as a red dashed line. Tyr193 at the dimer interface and residues important for E2 binding (Met140 or Arg181) are shown in stick representation. The linear fusion protein contains one substrate-binding site, two E2-binding sites, and two Tyr193 residues, one on each side of the dimerization interface. A schematic representation of the RNF4-RING fusion protein is shown on the right-hand side. **(b)** Substrate ubiquitylation activity of RNF4-RING linear fusion proteins, with mutations in full-length RNF4 and/or the RNF4 RING domain as indicated. Data are shown as mean \pm s.d. of duplicate reactions. The experiment was performed twice. The upper panel shows a SYPRO Orange-stained SDS-PAGE gel with purified RNF4-RING fusion proteins ($0.6 \mu\text{g}$). **(c)** Mutation of Tyr193 in the RING domain that does not bind E2 causes an increase in K_M and a decrease in k_{cat} . Michaelis-Menten kinetics were determined by varying concentration of the UbcH5a~Ub thioester. **(d)** Binding of the E2~ubiquitin oxyster to RNF4-RING fusion proteins correlates well with their ubiquitylation activities. A pull-down experiment was performed as in Fig. 4e.

Table 1

Data collection, phasing and refinement statistics

	SAD data set	data set used for refinement
Data collection		
Space group	P4 ₁ 32	P4 ₁ 32
Cell dimensions		
<i>a, b, c</i> (Å)	72.6, 72.6, 72.6	72.6, 72.6, 72.6
<i>α, β, γ</i> (°)	90.0, 90.0, 90.0	90.0, 90.0, 90.0
Wavelength (Å)	1.28	0.98
Resolution (Å)	40.00–1.70 (1.76–1.70) ^a	18.00–1.50 (1.55–1.50)
<i>R</i> _{sym}	0.079 (0.546)	0.062 (0.426)
<i>I</i> / <i>σI</i>	16.3 (4.4)	18.0 (2.9)
Completeness (%)	99.3 (100.0)	99.8 (100.0)
Redundancy	12.8 (13.0)	9.9 (7.3)
Refinement		
Resolution (Å)		18–1.5
No. reflections		10,391
<i>R</i> _{work} / <i>R</i> _{free}		0.168 / 0.197
No. atoms		
Protein		507
Zn ²⁺		2
Sucrose/SO ₄ ²⁻		23/10
Water		54
<i>B</i> -factors		
Protein		24
Zn ²⁺		20
Sucrose/SO ₄ ²⁻		25/46
Water		31
R.m.s deviations		
Bond lengths (Å)		0.009
Bond angles (°)		1.44

^aValues in parentheses are for highest-resolution shell. One crystal was used for each data set.